Simplified Voltage-Behind-Reactance Saturable Synchronous Machine Model for State-Variable-Based Transient Simulation Programs

F. Therrien, M. Chapariha, H. Atighechi, J. Jatskevich

***Abstract*—The accuracy and numerical efficiency of synchronous machine models are known to have a significant impact on power systems transient studies. In this paper, a new saturable synchronous machine model for state-variable-based transient simulation programs is proposed. The new model uses the voltage-behind-reactance formulation, which, unlike the standard *qd* models, allows a direct interface between the machine and any external network. The proposed model fully includes static and dynamic cross-saturation using the single saliency factor approach and allows easy incorporation of any number of *d*-axis damper windings and differential leakage inductances. The new model is shown to yield very high accuracy and improved numerical efficiency compared to the conventional indirectly interfaced *qd* models.**

***Keywords*: Saturation, state-variable-based, synchronous machine, transient simulation, voltage-behind-reactance.**

I. Introduction

The accurate and efficient modeling of synchronous machines (SMs) for power systems transient studies has been a subject of interest for many decades [1]–[5], [7]–[26]. Traditionally, SMs have been represented in transient programs by classical qd models, which are based on Park's two-reaction theory [1]. These models are very efficient and practical due to their time-independent decoupled inductances, simple equivalent circuits, and constant steady-state currents, voltages, and fluxes. However, interfacing of qd models with external networks is often problematic [2]. In particular, in state-variable-based simulation programs (e.g. MATLAB/Simulink, SimPowerSystems [3], PLECS [4], ASMG [5], etc.), the voltage-input, current-output formulation of the qd models does not permit their direct interfacing with series inductive elements or ideal switches [2]. A typical approach to solve this problem is to add a snubber at the machine's stator terminals. On the one hand, a small snubber resistance introduces a considerable error. On the other hand, a large snubber resistance significantly increases the numerical stiffness [6] of the state-space model.

An alternative method to overcome this interfacing issue is to use a phase-domain (PD) model [1], [7], [8]. Whereas this model lacks efficiency due to its time-varying coupled inductances, it can be directly interfaced to any external network. It is also believed to offer better absolute numerical stability, which can be useful for real-time simulations [8]. In 1998, a magnetically linear voltage-behind-reactance (VBR) SM model was introduced [9], which was shown to be considerably more efficient than the PD model. In the VBR model, the stator is represented in the abc phase coordinates as a voltage source behind time-varying impedance, thus also allowing direct interfacing with any external system. As opposed to the PD model, the rotor dynamics are represented by state-space equations with flux linkages as state variables, yielding better scaled eigenvalues, and consequently a more efficient solution. Numerical approximations and techniques have also been proposed to obtain constant equivalent stator impedance in the magnetically linear VBR SM model [10]–[12], further improving its efficiency. Magnetic saturation was eventually introduced in VBR SM models, first in the d-axis only [13], and later in both axes (including cross-saturation) [14], [15].

The existence of magnetic saturation in SMs is a duly recognized fact. Much literature has been devoted to modeling magnetic saturation in SM models for transient studies; yet, numerous conflicting opinions remain today [13]–[22]. For round rotor machines, a common approach is to apply saturation to the main flux (thus including cross-saturation) as a function of the d-axis saturation curve [1], [3], [4], which can be easily obtained from the standard open-circuit test. However, practical experiments have shown that the q-axis may, in some cases, saturate more heavily than the d-axis [16]. For salient-pole SMs, a common assumption is to neglect q-axis saturation, and thus cross-saturation altogether [3], [13], [16]. The usual reasoning behind this hypothesis is that the path of the q-axis flux is largely in air [16]. Finite-element analysis (FEA) [17] and experimental studies [18], [19] have shown however that cross-saturation has a considerable effect even for salient-pole machines. Ideally, a two-factor saturation approach, such as the one originally presented in [20] (or later adapted in [14]), would be preferred for both round rotor and salient-pole machines. In reality, for system transient studies, only the d-axis saturation curve is typically known [21].

This research was supported by the Natural Science and Engineering Research Council (NSERC) of Canada.

F. Therrien, M. Chapariha, H. Atighechi, and J. Jatskevich are with the Department of Electrical and Computer Engineering, The University of British Columbia, Vancouver, BC, V6T 1Z4, Canada (e-mail: {francist,mehrdadc,hamida,jurij}@ece.ubc.ca).

Paper submitted to the International Conference on Power Systems Transients (IPST2013) in Vancouver, Canada July 18-20, 2013.

Therefore, the single saliency factor approach [4], [19], [21], in which q-axis saturation and cross-saturation are taken into account (solely based on the d-axis saturation curve) is a very practical and appealing technique.

Another issue of debate in SM modeling is the composition of the equivalent d-axis rotor circuit [1], [23]–[25]. Some authors argued about the necessity, or lack thereof, of including so-called differential leakage inductances [23]–[25], which link the fluxes of some or all rotor windings, but not of the stator winding. Whereas the physical meaning of such inductances is usually accepted [24], [25], linear circuit theory showed that the sole differential leakage inductance of 2nd order rotor circuits can be equated to zero [23], [24]. However, this is done by changing the stator leakage and magnetizing inductances from physical to fictitious values, which in turn makes the inclusion of leakage and main flux saturation more complicated. It is also not clear if this can be done for 3rd order (or higher) rotor circuits. It is argued in [1] that simply neglecting the differential leakage inductance yields satisfactory results for most cases. This point of view is commonly accepted, as numerous saturable SM models do not include differential leakage inductances [1], [3], [4], [13], [21]. To satisfy the modeling needs of various users, a general model should handle equivalent rotor circuits with or without differential leakage inductances. One such model is presented in [14], wherein the rotor is represented by an arbitrary transfer function. This approach is very flexible, but has the disadvantage of being highly complicated.

This paper develops a straightforward and easy-to-use saturable VBR SM model for state-variable-based transient programs. Magnetic saturation is represented explicitly using the single saliency factor approach, while fully incorporating dynamic and static cross-saturation. The proposed model is derived so that the equivalent d-axis rotor circuit (made of passive circuit elements) can include as many damper windings as necessary and may or may not have differential leakage inductances. Moreover, as opposed to [14], the equivalent stator resistance matrix is constant and diagonal, further simplifying the model.

II. Representation of Magnetic Saturation

The **m**agneto**m**otive **f**orce (MMF) and the main flux of anisotropic machines are not aligned [20], [21]. To facilitate the modeling of cross-saturation in such machines, a common approach is to introduce a fictitious equivalent isotropic machine [20], [21], wherein the MMF and the main flux are aligned and therefore a unique magnetic characteristic exists. The magnetizing current i_m and main flux λ_m of the resulting isotropic machine are related to their q-and d-axis projections as

$$\lambda_m = \sqrt{\lambda_{md}^2 + \left(\frac{\lambda_{mq}}{m}\right)^2} \tag{1}$$

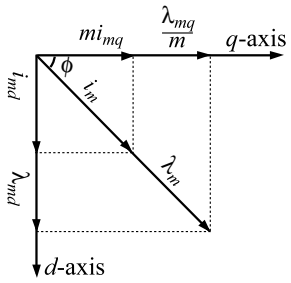

Fig. 1. Vector diagram presenting the magnetizing current i_m and main flux λ_m of the equivalent isotropic synchronous machine.

$$i_m = \sqrt{i_{md}^2 + \left(mi_{mq}\right)^2} \ . \tag{2}$$

A vector diagram depicting the re-scaled projections of the currents and fluxes in the q-axis is shown in Fig. 1. For the two-factor saturation approach, m is a saturation-dependent parameter [20]. However, in most practical cases, not enough data is available to apply the two-factor saturation approach, and the single saliency factor method [21] is preferred (as in this paper). In this case, m is assumed to remain constant and is defined as

$$m = \sqrt{\frac{L_{mqu}}{L_{mdu}}} = \sqrt{\frac{L_{mqs}}{L_{mds}}} \tag{3}$$

where L_{mqu}, L_{mdu}, L_{mqs}, and L_{mds} are the unsaturated and saturated q- and d-axes magnetizing inductances, respectively. In other words, (3) assumes that the q- and d-axis saturate at the same level in all conditions. This approach works for both salient-pole and round rotor machines; for the latter, m simply tends towards 1. Finally, in the single saliency factor approach, the d-axis saturation characteristic is applied to the resulting main flux, (1). Two-factor saturation approaches are herein excluded from further consideration; however, only minor modifications to the proposed model would be required to incorporate these more general methods.

III. Synchronous Machine Dynamic Model

A. Equivalent Circuits

In this paper, a SM with M damper windings in the q-axis and N damper windings in the d-axis is considered; its equivalent d- and q-axes circuits in the rotor reference frame are depicted in Fig. 2. The zero-sequence circuit can be found in [1] and is not presented here due to space constraints. Here, all elements are referred to the stator, and motor sign convention is used. As it can be observed in Fig. 2a), for generality [25], the equivalent d-axis rotor circuit possesses as many differential leakage inductances, denoted L_{lkfdj}, as it has d-axis damper windings. It is assumed that none, some, or all of these inductances may be set to zero as long as all the winding leakage inductances (L_{lkdj} and L_{lfd}) are present.

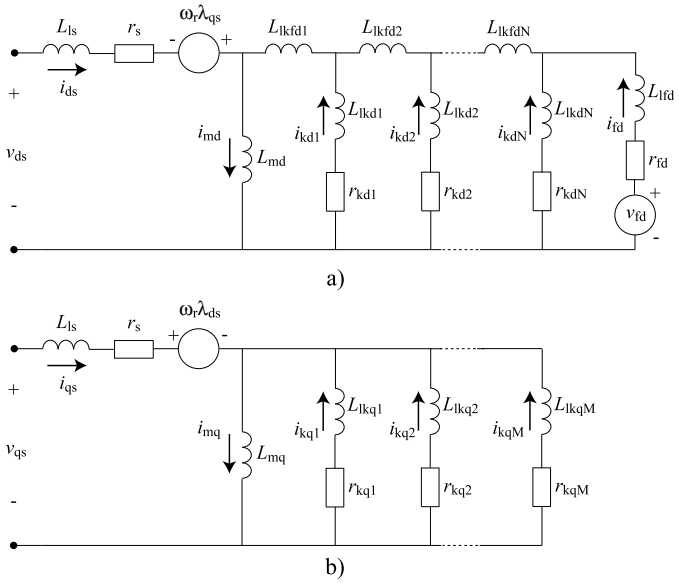

Fig. 2. Equivalent circuits of the synchronous machine: a) the *d*-axis; and b) the *q*-axis.

B. Dynamic Equations in qd Coordinates

The dynamic equations of the equivalent networks of Fig. 2 (with the addition of the zero-sequence circuit [1]) can be easily derived. The resulting voltage equations are

$$v_{qs} = r_s i_{qs} + \omega_r \lambda_{ds} + p\lambda_{qs} \tag{4}$$

$$v_{ds} = r_s i_{ds} - \omega_r \lambda_{qs} + p\lambda_{ds} \tag{5}$$

$$v_{0s} = r_s i_{0s} + p\lambda_{0s} \tag{6}$$

$$0 = r_{kqj} i_{kqj} + p\lambda_{kqj}, \quad j = 1,2,...,M. \tag{7}$$

$$v_{drj} = r_{drj} i_{drj} + p\lambda_{drj}, \quad j = 1,2,...,N,N+1. \tag{8}$$

where

$$\mathbf{f}_{dr} = \begin{bmatrix} f_{kd1} & f_{kd2} & \cdots & f_{kdN} & f_{fd} \end{bmatrix}^T. \tag{9}$$

Here, f may represent v, r, i, or λ. The corresponding flux linkages are defined as

$$\lambda_{qs} = L_{ls} i_{qs} + \lambda_{mq} \tag{10}$$

$$\lambda_{ds} = L_{ls} i_{ds} + \lambda_{md} \tag{11}$$

$$\lambda_{0s} = L_{ls} i_{0s} \tag{12}$$

$$\lambda_{kqj} = L_{lkqj} i_{kqj} + \lambda_{mq}, \quad j = 1,2,...,M. \tag{13}$$

$$\boldsymbol{\lambda}_{dr} = \mathbf{L}_{ldr} \mathbf{i}_{dr} + \lambda_{md} \mathbf{u} \tag{14}$$

where $\mathbf{u} = \begin{bmatrix} 1 & 1 & \cdots & 1 & 1 \end{bmatrix}^T$ and

$$\mathbf{L}_{ldr} = \tag{15}$$

$$\begin{bmatrix} L_{lkd1} + L_{lkfd1} & L_{lkfd1} & \cdots & L_{lkfd1} & L_{lkfd1} \\ L_{lkfd1} & L_{lkd2} + \sum_{j=1}^{2} L_{lkfdj} & \cdots & \sum_{j=1}^{2} L_{lkfdj} & \sum_{j=1}^{2} L_{lkfdj} \\ \vdots & \vdots & \ddots & \vdots & \vdots \\ L_{lkfd1} & \sum_{j=1}^{2} L_{lkfdj} & \cdots & L_{lkdN} + \sum_{j=1}^{N} L_{lkfdj} & \sum_{j=1}^{N} L_{lkfdj} \\ L_{lkfd1} & \sum_{j=1}^{2} L_{lkfdj} & \cdots & \sum_{j=1}^{N} L_{lkfdj} & L_{lfd} + \sum_{j=1}^{N} L_{lkfdj} \end{bmatrix}.$$

It can be observed that as long as the winding leakage inductances are non-zero, (15) will remain non-singular independently of the existence of differential leakage inductances. Finally, the magnetizing fluxes are given by

$$\lambda_{mq} = L_{mq}(\lambda_m) i_{mq} = L_{mq}(\lambda_m) \left(i_{qs} + \sum_{j=1}^{M} i_{kqj} \right) \tag{16}$$

$$\lambda_{md} = L_{md}(\lambda_m) i_{md} = L_{md}(\lambda_m) \left(i_{ds} + \sum_{j=1}^{N+1} i_{drj} \right) \tag{17}$$

where the relationship between $L_{mq}(\lambda_m)$ and $L_{md}(\lambda_m)$ was defined in (3).

C. Voltage-Behind-Reactance Formulation

Rotor flux linkages are typically selected as state variables in SM VBR models [9]. However, in order to derive an explicit SM model incorporating main flux saturation, it is convenient to choose the magnetizing fluxes $\boldsymbol{\lambda}_{mqd}$ as state variables [13]–[15]. Consequently, one pair of rotor flux linkages has to be removed from the equivalent rotor subsystem state variable vector, which thus becomes

$$\mathbf{x}_r = \begin{bmatrix} \lambda_{mq} & \lambda_{md} & \lambda_{kq2} & \cdots & \lambda_{kqM} & \lambda_{dr2} & \cdots & \lambda_{dr(N+1)} \end{bmatrix}^T. \tag{18}$$

To start the derivation of the model, it is useful to first define $\Gamma_{m\sigma}(\lambda_m) \equiv 1/L_{m\sigma}(\lambda_m)$, where σ denotes the axis (q or d). Then, differentiating (16) and (17) yields

$$p\begin{bmatrix} i_{mq} \\ i_{md} \end{bmatrix} = \begin{bmatrix} p\Gamma_{mq}(\lambda_m)\lambda_{mq} \\ p\Gamma_{md}(\lambda_m)\lambda_{md} \end{bmatrix} + \begin{bmatrix} \Gamma_{mq}(\lambda_m) p\lambda_{mq} \\ \Gamma_{md}(\lambda_m) p\lambda_{md} \end{bmatrix} \tag{19}$$

which, using the chain rule, can be rewritten as [14]

$$p\begin{bmatrix} i_{mq} \\ i_{md} \end{bmatrix} = \boldsymbol{\Gamma}_{mi}(\boldsymbol{\lambda}_{mqd}) p\begin{bmatrix} \lambda_{mq} \\ \lambda_{md} \end{bmatrix} \tag{20}$$

where

$$\boldsymbol{\Gamma}_{mi}(\boldsymbol{\lambda}_{mqd}) = \begin{bmatrix} \dfrac{d\Gamma_{mq}(\lambda_m)}{d\lambda_m} \dfrac{\lambda_{mq}^2}{m^2 \lambda_m} + \Gamma_{mq}(\lambda_m) & \dfrac{d\Gamma_{mq}(\lambda_m)}{d\lambda_m} \dfrac{\lambda_{mq}\lambda_{md}}{\lambda_m} \\ \dfrac{d\Gamma_{md}(\lambda_m)}{d\lambda_m} \dfrac{\lambda_{mq}\lambda_{md}}{m^2 \lambda_m} & \dfrac{d\Gamma_{md}(\lambda_m)}{d\lambda_m} \dfrac{\lambda_{md}^2}{\lambda_m} + \Gamma_{md}(\lambda_m) \end{bmatrix} \tag{21}$$

and

$$p\begin{bmatrix} i_{mq} \\ i_{md} \end{bmatrix} = p\begin{bmatrix} i_{qs} \\ i_{ds} \end{bmatrix} + p\begin{bmatrix} \sum_{j=1}^{M} i_{kqj} \\ \sum_{j=1}^{N+1} i_{drj} \end{bmatrix}. \tag{22}$$

At this point, it is necessary to define the rotor currents (auxiliary variables) as a function of the rotor and magnetizing flux linkages. Solving (13) for q-axis rotor currents gives

$$i_{kqj} = \frac{\lambda_{kqj} - \lambda_{mq}}{L_{lkqj}}, \quad j = 1,2,...,M. \tag{23}$$

whereas the d-axis rotor currents are obtained from (14):

$$\mathbf{i}_{dr} = \mathbf{L}_{ldr}^{-1} (\boldsymbol{\lambda}_{dr} - \lambda_{md} \mathbf{u}). \tag{24}$$

Since $\mathbf{L}_{ldr}$ is a constant matrix, it only needs to be inverted in the initialization stage. Moreover, if the coupling between all d-axis windings is assumed equal, i.e. $L_{lkfdj} = 0$, $j = 1,...,N$, matrices $\mathbf{L}_{ldr}$ and $\mathbf{L}_{ldr}^{-1}$ will be diagonal, hence decreasing the

overall computational cost of the model.

Taking the time derivative of (23) and (24), substituting the resulting equations into (20), after some algebraic manipulations, the magnetizing flux state equations are rewritten as [14]

$$p\begin{bmatrix}\lambda_{mq}\\ \lambda_{md}\end{bmatrix}=\begin{bmatrix}L_{mqq} & L_{mqd}\\ L_{mqd} & L_{mdd}\end{bmatrix}\left(p\begin{bmatrix}i_{qs}\\ i_{ds}\end{bmatrix}+p\begin{bmatrix}\sum_{j=1}^{M}\frac{\lambda_{kqj}}{L_{lkqj}}\\ \sum_{j=1}^{N+1}\left(\sum_{i=1}^{N+1}L_{ldr}^{-1}(j,i)\lambda_{dri}\right)\end{bmatrix}\right) \quad (25)$$

where

$$\begin{bmatrix}L_{mqq} & L_{mqd}\\ L_{mqd} & L_{mdd}\end{bmatrix}^{-1}=\boldsymbol{\Gamma}_{mi}(\boldsymbol{\lambda}_{mqd})+\begin{bmatrix}\sum_{j=1}^{M}\frac{1}{L_{lkqj}} & 0\\ 0 & \sum_{j=1}^{N+1}\left(\sum_{i=1}^{N+1}L_{ldr}^{-1}(j,i)\right)\end{bmatrix} \quad (26)$$

and where $L_{ldr}^{-1}(j,i)$ refers to the element found in the j th row and i th column of $\mathbf{L}_{ldr}^{-1}$.

To obtain an explicit model, (25) needs to be written as a function of state variables and inputs. Substituting (10), (11), and (25) into (4) and (5) and solving for $p\mathbf{i}_{qds}$ yields

$$p\begin{bmatrix}i_{qs}\\ i_{ds}\end{bmatrix}=L_{eq}^{-1}\begin{bmatrix}(L_{ls}+L_{mqq})^{-1}\left(y_q-(L_{ls}+L_{mdd})^{-1}L_{mqd}\,y_d\right)\\ (L_{ls}+L_{mdd})^{-1}\left(y_d-(L_{ls}+L_{mqq})^{-1}L_{mqd}\,y_q\right)\end{bmatrix} \quad (27)$$

where

$$L_{eq}=\left(1-\frac{L_{mqd}^2}{(L_{ls}+L_{mqq})(L_{ls}+L_{mdd})}\right) \quad (28)$$

$$\begin{bmatrix}y_q\\ y_d\end{bmatrix}=\begin{bmatrix}v_{qs}-r_s i_{qs}-\omega_r(L_{ls}i_{ds}+\lambda_{md})-e_q\\ v_{ds}-r_s i_{ds}+\omega_r(L_{ls}i_{qs}+\lambda_{mq})-e_d\end{bmatrix} \quad (29)$$

and

$$\begin{bmatrix}e_q\\ e_d\end{bmatrix}=\begin{bmatrix}L_{mqq} & L_{mqd}\\ L_{mqd} & L_{mdd}\end{bmatrix}p\begin{bmatrix}\sum_{j=1}^{M}\frac{\lambda_{kqj}}{L_{lkqj}}\\ \sum_{j=1}^{N+1}\left(\sum_{i=1}^{N+1}L_{ldr}^{-1}(j,i)\lambda_{dri}\right)\end{bmatrix}. \quad (30)$$

Next, the rotor flux linkages time derivatives are written as a function of state variables and inputs. Solving for $p\lambda_{kqj}$ and $p\lambda_{drj}$ in (7) and (8), respectively, we obtain

$$p\lambda_{kqj}=-r_{kqj}i_{kqj},\quad j=1,2,...,M. \quad (31)$$

$$p\lambda_{drj}=v_{drj}-r_{drj}i_{drj},\quad j=1,2,...,N,N+1. \quad (32)$$

where the rotor currents are related to rotor flux linkages and magnetizing fluxes by (23) and (24). Due to the choice of state variables [see (18)], (31) and (32) will only be state equations (and thus integrated) for $j=2,3,...,M$ and $j=2,3,...N,N+1$, respectively. The final step consists in eliminating the auxiliary algebraic variables λ_{kq1} and λ_{dr1}. Substituting (23) and (24) in (16) and (17), respectively, after some algebraic manipulations, λ_{kq1} and λ_{dr1} are related to state variables and inputs by

$$\lambda_{kq1}=L_{lkq1}\left(\lambda_{mq}\left(\Gamma_{mq}(\lambda_m)+\sum_{j=1}^{M}\frac{1}{L_{lkqj}}\right)-\sum_{j=2}^{M}\frac{\lambda_{kqj}}{L_{lkqj}}-i_{qs}\right) \quad (33)$$

$$\lambda_{dr1}=\left(\frac{1}{\sum_{j=1}^{N+1}L_{ldr}^{-1}(j,1)}\right)\left(\lambda_{md}\left(\Gamma_{md}(\lambda_m)+\sum_{j=1}^{N+1}L_{ldr}^{-1}(j,1)\right)-\sum_{j=1}^{N+1}\left(\sum_{i=2}^{N+1}L_{ldr}^{-1}(j,i)(\lambda_{dri}-\lambda_{md})\right)-i_{ds}\right). \quad (34)$$

Having derived the necessary equations for the equivalent rotor subsystem, the stator is henceforth considered. First, inserting (10) and (11) into (4) and (5) yields [14]

$$\begin{bmatrix}v_{qs}\\ v_{ds}\end{bmatrix}=r_s\begin{bmatrix}i_{qs}\\ i_{ds}\end{bmatrix}+\omega_r\begin{bmatrix}(L_{ls}i_{ds}+\lambda_{md})\\ -(L_{ls}i_{qs}+\lambda_{mq})\end{bmatrix}+L_{ls}p\begin{bmatrix}i_{qs}\\ i_{ds}\end{bmatrix}+p\begin{bmatrix}\lambda_{mq}\\ \lambda_{md}\end{bmatrix}. \quad (35)$$

Then, substituting (12) into (6), (25) into (35), and merging the two resulting sets of equations together, we obtain

$$\begin{bmatrix}v_{qs}\\ v_{ds}\\ 0\end{bmatrix}=r_s\begin{bmatrix}i_{qs}\\ i_{ds}\\ i_{0s}\end{bmatrix}+\omega_r\begin{bmatrix}-L_{mqd} & (L_{ls}+L_{mqq}) & 0\\ -(L_{ls}+L_{mdd}) & L_{mqd} & 0\\ 0 & 0 & 0\end{bmatrix}\begin{bmatrix}i_{qs}\\ i_{ds}\\ i_{0s}\end{bmatrix}+\begin{bmatrix}(L_{mqq}+L_{ls}) & L_{mqd} & 0\\ L_{mqd} & (L_{mdd}+L_{ls}) & 0\\ 0 & 0 & L_{ls}\end{bmatrix}p\begin{bmatrix}i_{qs}\\ i_{ds}\\ i_{0s}\end{bmatrix}+\begin{bmatrix}e_q''\\ e_d''\\ 0\end{bmatrix} \quad (36)$$

where

$$\begin{bmatrix}e_q''\\ e_d''\end{bmatrix}=\omega_r\begin{bmatrix}L_{mqd} & -L_{mqq}\\ L_{mdd} & -L_{mqd}\end{bmatrix}\begin{bmatrix}i_{qs}\\ i_{ds}\end{bmatrix}+\omega_r\begin{bmatrix}\lambda_{md}\\ -\lambda_{mq}\end{bmatrix}+\begin{bmatrix}e_q\\ e_d\end{bmatrix}. \quad (37)$$

Applying Park's inverse transformation [1] to (36) gives the final machine-network interfacing equation in *abc* phase coordinates:

$$\mathbf{v}_{abcs}=r_s\mathbf{i}_{abcs}+L_{ls}p\mathbf{i}_{abcs}+\mathbf{L}_s(\theta_r)p\mathbf{i}_{abcs}+\mathbf{e}_{abcs}''. \quad (38)$$

Here, $\mathbf{e}_{abcs}''=\mathbf{K}_s^{-1}\begin{bmatrix}e_q'' & e_d'' & 0\end{bmatrix}^T$, $\mathbf{f}_{abcs}=\begin{bmatrix}f_{as} & f_{bs} & f_{cs}\end{bmatrix}^T$ (where f may represent v or i), $\mathbf{K}_s$ is Park's transformation matrix [1], and

$$\mathbf{L}_s=-L_a\begin{bmatrix}-1 & 0.5 & 0.5\\ 0.5 & -1 & 0.5\\ 0.5 & 0.5 & -1\end{bmatrix}+\begin{bmatrix}L(\theta_r) & L(\theta_r+120^\circ) & L(\theta_r-120^\circ)\\ L(\theta_r+120^\circ) & L(\theta_r-120^\circ) & L(\theta_r)\\ L(\theta_r-120^\circ) & L(\theta_r) & L(\theta_r+120^\circ)\end{bmatrix} \quad (39)$$

$$L_a=\frac{L_{mqq}+L_{mdd}}{3},\ L_b=\frac{L_{mqq}-L_{mdd}}{3},\ L_c=\frac{2}{3}L_{mqd} \quad (40)$$

$$L(\varphi)=L_b\cos(2\varphi)+L_c\sin(2\varphi). \quad (41)$$

Eq. (38) shows that unlike the model presented in [14], the proposed equivalent stator circuit has a constant diagonal resistance matrix. This property was achieved by adding and subtracting certain speed voltage terms in $\mathbf{e}_{abcs}''$.

IV. Computer Studies

To validate the proposed approach and assess its perfor-

mance, the saturable SM VBR model (Section III-C) has been implemented in MATLAB/Simulink using the PLECS toolbox [4]. A 202-MVA salient-pole synchronous generator (SG) with one q-axis and one d-axis damper windings, and one differential leakage inductance (denoted by L_{lkdf1}), is considered [22]. Machine parameters and saturation data are listed in Appendices A and B, respectively. For comparison, a standard qd SM model has also been implemented in the MATLAB/Simulink environment. Saturation is therein represented using the Explicit Flux Correction approach [26] (with minor modifications to take into account L_{lkdf1}), which was found to offer the best combination of accuracy and numerical efficiency among saturable qd models. The simulations were executed on a PC with 2.8GHz Intel CPU and 4GB of RAM.

A. Model Verification

The consistency of the proposed SM VBR model is first verified by comparing it to the qd SM model for a simple single machine-infinite bus system. As stator voltages are system inputs, the qd model and the infinite bus are directly interfaced. In this study, the SG is assumed to be initially in steady state with nominal field and stator voltages, and a 0.9 pu mechanical torque. At $t = 0.5$ s, the stator voltage is increased to 1.05 pu. Simulink's robust and accurate ode45 solver is used for this case study. Its settings, which were chosen as to minimize numerical errors, are as follows: maximum and minimum step sizes of 10^{-4} s and 10^{-8} s, respectively, and absolute and relative tolerances of 10^{-5}. The predicted transients in q-axis stator current i_{qs} and rotor angle δ are presented in Fig. 3 and Fig. 4, respectively. No difference is observed between the VBR and qd models, which validates the consistency of the proposed approach. The 2-norm relative error [27] between the solution trajectories produced by the two models is found to be less than 0.01% for both i_{qs} and δ, further verifying the model's consistency.

B. Comparison between the VBR and qd Models

To assess the accuracy and efficiency of the proposed model in more practical situations, a small network, presented in Fig. 5, is considered. In this network, a SG is connected through a short cable to the low voltage (LV) side of a step-up transformer, while a three-phase Thévenin equivalent source representing the remaining ac subsystem is connected to the high voltage (HV) side. The system parameters are summarized in Appendix C. The selection of a small network for this case study gives more insight into the machine model, as the accuracy and the computational cost of the solution can be traced back directly to its numerical properties. Since the machine is in series with inductive elements, the qd model cannot be interfaced directly with the network, and a snubber (herein resistive) must be used. Two instances of the qd model with different values of resistance for the snubber are used: $R_{sn} = 50\,\Omega$ for model $qd1$, and $R_{sn} = 1\,\Omega$ for model $qd2$.

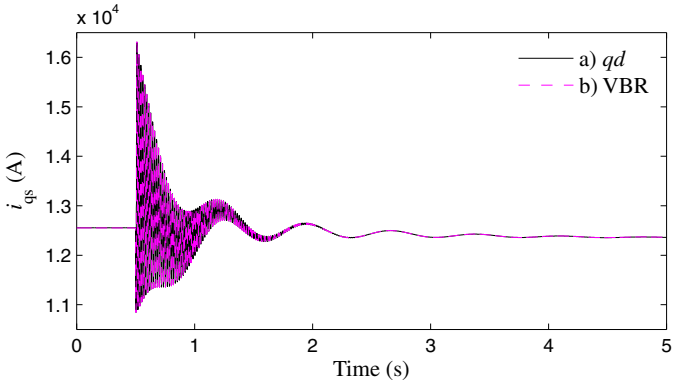

Fig. 3. Stator current i_{qs} following a step increase in stator voltage

.

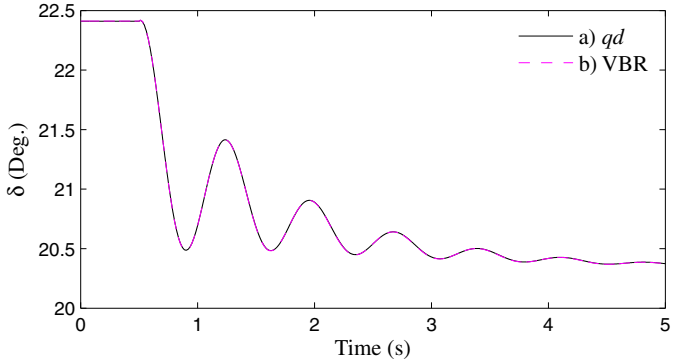

Fig. 4. Rotor angle δ following a step increase in stator voltage.

In this study, the SG is initially in steady state with mechanical torque of 0.9 pu. The source voltage is initially set to 1 pu, and the machine field voltage is set to 1.5 pu. At $t = 0.2$ s, a balanced three-phase fault is simulated by instantly decreasing the source voltage to 0.5 pu. The fault is cleared 6 cycles later, and the source returns immediately to its pre-fault value. A reference solution is obtained by simulating this scenario using the VBR model and the ode45 solver with very stringent settings (max. and min. step sizes of 10^{-5} s and 10^{-8} s, respectively, and absolute and relative tolerances of 10^{-6}). Three models are compared: $qd1$, $qd2$, and the proposed VBR. Due to the numerical stiffness caused by the snubber, the stiffly-stable ode15s solver is used with the following settings: max. and min. step sizes of 10^{-3} s and 10^{-8} s, respectively, and absolute and relative tolerances of 10^{-4}.

The predicted transient in q-axis stator current i_{qs} is shown in Fig. 6. For better clarity, a magnified view of i_{qs} is reproduced in Fig. 7. The transients in d-axis magnetizing flux λ_{md} and electromagnetic torque T_e are also plotted in Fig. 8 and Fig. 9, respectively. These figures show that the proposed VBR and $qd1$ models yield solutions

indistinguishable from the reference. However, the $qd2$ model generates a noticeable error, which is caused by the use of a relatively small snubber. Similar observations are made when computing the 2-norm relative errors of the solution trajectories of each model with respect to the reference solutions for i_{qs}, λ_{md}, and T_e [see Table I]. As it can be seen in Table I, all errors are smaller than 0.1% for the $qd1$ and VBR models, whereas large errors, as high as 3.94%, exist when using the $qd2$ model.

To quantify the efficiency of the proposed approach, the number of time steps taken by each model and their overall simulation time for this study are summarized in Table I. The VBR model requires only 1,498 time steps, as opposed to 7,934 and 2,050 for $qd1$ and $qd2$, respectively. This is due to the VBR model's well-scaled eigenvalues [9]. Even the $qd2$ model, with the smaller snubber, yields a numerically stiffer problem. However, despite the fewer number of time steps taken, the proposed VBR model is significantly slower (0.945 s) than the $qd2$ model (0.339 s), while still being faster than the $qd1$ model (1.206 s), which gave similar accuracy. It is clear from these results that the main caveat of the proposed saturable VBR model lies in its time-varying equivalent stator inductance, which requires the reformulation of the state model at every time step and thus considerably decreases its efficiency [10]. Its flop count is also higher than those of the most efficient qd models. Nonetheless, for a given accuracy, the VBR model is shown to be more efficient, i.e. faster, than the corresponding indirectly interfaced qd model. The proposed model's ability to yield very accurate and stable solutions for large time steps is particularly valuable when simulating power converters with low switching frequencies [14] or average-value models (AVMs) [28].

TABLE I
ACCURACY AND EFFICIENCY OF THE PROPOSED MODEL

		$qd1$	$qd2$	VBR
2-norm relative error	i_{qs}	0.08%	3.70%	0.02%
	λ_{md}	0.07%	3.94%	0.02%
	T_e	0.01%	0.86%	0.003%
Number of time steps		7.934	2,050	1,498
Simulation CPU time		1.206s	0.339s	0.945s

V. CONCLUSIONS

A simplified saturable synchronous machine (SM) model using a voltage-behind-reactance (VBR) formulation with a generalized equivalent d-axis rotor circuit made of passive components is presented. The proposed model fully incorporates static and dynamic cross-saturation using the single saliency factor approach. The new model can be directly interfaced to any external network, including series inductive elements. The proposed model is also derived as to allow the presence (or lack thereof) of any amount of differential

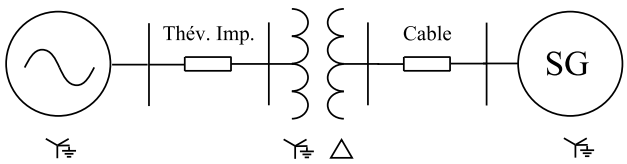

Fig. 5 Small network for the second case study.

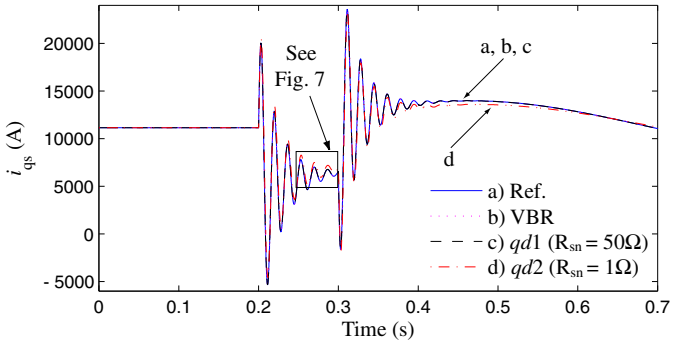

Fig. 6. Stator current i_{qs} for a three-phase fault.

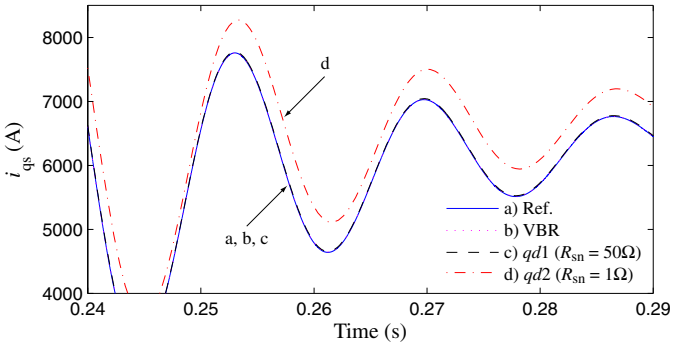

Fig. 7. Magnified view of the stator current i_{qs} during the three-phase fault.

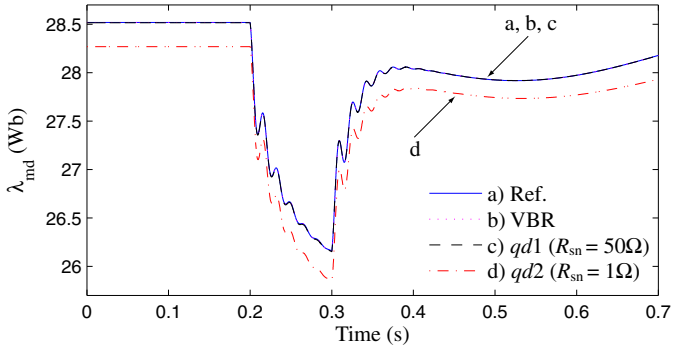

Fig. 8. Magnetizing flux λ_{md} for a three-phase fault.

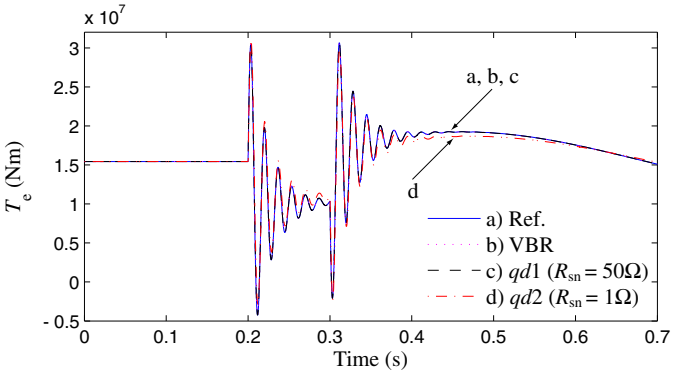

Fig. 9. Electromagnetic torque T_e for a three-phase fault.

leakage inductances. The validity of the proposed model is first confirmed in a simple single machine-infinite bus case study. The paper also demonstrates that the proposed model requires significantly fewer time steps than an indirectly interfaced classical *qd* model that achieves a similar accuracy.

VI. Appendix

A) Synchronous generator parameters (all parameters are referred to the stator) [22]:

$202\,\text{MVA}$, $13.8\,\text{kV}$, $60\,\text{Hz}$, 64 poles, $J = 20\cdot 10^6\,\text{J}\cdot\text{s}^2$,
$r_s = 0.0019\,\Omega$, $L_{ls} = 0.495\,\text{mH}$, $r_{fd} = 0.500\,\text{m}\Omega$,
$L_{lfd} = 0.320\,\text{mH}$, $L_{lkfd1} = -0.045\,\text{mH}$, $r_{kd1} = 0.0071\,\Omega$,
$L_{lkd1} = 0.086\,\text{mH}$, $r_{kq1} = 0.0065\,\Omega$, $L_{lkq1} = 0.038\,\text{mH}$,
$L_{md} = 2.27\,\text{mH}$, $L_{mq} = 0.545\,\text{mH}$.

B) Synchronous machine saturation curve (peak values):

λ_m (Wb)	10.7	16.2	20.2	24.3	26.4	28.0	29.3	29.9
i_m (kA)	4.757	7.245	9.148	11.71	13.39	15.37	18.30	20.49

C) System parameters:

Transformer: $S_{base} = 300\,\text{MVA}$, $V_H = 230\,\text{kV}$, $V_L = 13.8\,\text{kV}$,
$Z_0 = Z_1 = 2 + j8\ \%$.

Cable: $Z_0 = 0.015 + j0.045\,\Omega$, $Z_1 = 0.005 + j0.015\,\Omega$.

Thév. Eq.: $V_{nom} = 230\,\text{kV}$, $Z_0 = 5 + j23.1\,\Omega$, $Z_1 = 3 + j18.5\,\Omega$.

VII. References

[1] P. C. Krause, O. Wasynczuk, and S. D. Sudhoff, *Analysis of Electric Machinery and Drive Systems*, 2nd Edition, Piscataway, NJ: IEEE Press, 2002.

[2] L. Wang et al., "Methods of interfacing rotating machine models in transient simulation programs," *IEEE Trans. Power Deliv*., vol. 25, no. 2, pp. 891-903, Apr. 2010.

[3] "*SimPowerSystems R2009a – User's Guide*," The MathWorks, Inc., Natick, MA, 2009. [Online]. Available: www.mathworks.com.

[4] "*Piece-wise Linear Electrical Circuit Simulation (PLECS) User Manual Version 3.2*," Plexim GmbH, 2012. [Online]. Available: www.plexim.com.

[5] *"Automated State Model Generator (ASMG) Reference Manual,"* P. C. Krause and Associates, Inc., West Lafayette, IN, 2002.

[6] U. M. Ascher and L. R. Petzold, *Computer Methods for Ordinary Differential Equations and Differential-Algebraic Equations*, Philadelphia, PA: SIAM, 1998.

[7] P. Subramaniam and O. P. Malik, "Digital simulation of a synchronous generator in the direct-phase quantities," *Proc. Inst. Elect. Eng*., vol. 118, no. 1, pp. 153-160, Jan. 1971.

[8] J. R. Marti and K. W. Louie, "A phase-domain synchronous generator model including saturation effects," *IEEE Trans. Power Syst*., vol. 12, no. 1, pp. 222-229, Feb. 1997.

[9] S. D. Pekarek, O. Wasynczuk, and H. J. Hegner, "An efficient and accurate model for the simulation and analysis of synchronous machine/converter systems," *IEEE Trans. Energy Convers.*, vol. 13, no. 1, pp. 42-48, Mar. 1998.

[10] S. D. Pekarek and E. A. Walters, "An accurate method of neglecting dynamic saliency of synchronous machines in power electronic based systems," *IEEE Trans. Energy Convers*., vol. 14, no. 4, pp. 1177-1183, Dec. 1999.

[11] S. D. Pekarek, M. T. Lemanski, and E. A. Walters, "On the use of singular perturbations to neglect the dynamic saliency of synchronous machines," *IEEE Trans. Energy Convers.*, vol. 17, no. 3, pp. 385-391, Sep. 2002.

[12] M. Chapariha, L. Wang, J. Jatskevich, H. W. Dommel, and S. D. Pekarek, "Constant-parameter RL-branch equivalent circuit for interfacing AC machine models in state-variable-based simulation packages," *IEEE Trans. Energy Convers.*, vol. 27, no. 3, pp. 634-645, Sep. 2012.

[13] S. D. Pekarek, E. A. Walters, and B. T. Kuhn, "An efficient and accurate method of representing magnetic saturation in physical-variable models of synchronous machines," *IEEE Trans. Energy Convers.*, vol. 14, no. 1, pp. 72-79, Mar. 1999.

[14] D. C. Aliprantis, O. Wasynczuk, and C. D. Rodríguez Valdez, "A voltage-behind-reactance synchronous machine model with saturation and arbitrary rotor network representation," *IEEE Trans. Energy Convers.*, vol. 23, no. 2, pp. 499-508, Jun. 2008.

[15] A. M. Cramer, B. P. Loop, and D. C. Aliprantis, "Synchronous machine model with voltage-behind-reactance formulation of stator and field windings," *IEEE Trans. Energy Convers.*, vol. 27, no. 2, pp. 391-402, Jun. 2012.

[16] P. Kundur, *Power System Stability and Control*, New York: McGraw-Hill, 1994, ch. 3.

[17] D. C. MacDonald, A. B. J. Reece, and P. J. Turner, "Turbine-generator steady-state reactances," *IEE Proc. C.,* vol. 132, no. 3, pp. 101-108, May 1985.

[18] A. M. El-Serafi, A. S. Abdallah, M. K. El-Sherbiny, and E. H. Badawy, "Experimental study of the saturation and the cross-magnetizing phenomenon in saturated synchronous machines," *IEEE Trans. Energy Convers*., vol. 3, no. 4, pp. 815-823, Dec. 1988.

[19] A. M. El-Serafi and N. C. Kar, "Methods for determining the intermediate-axis saturation characteristics of salient-pole synchronous machines from the measured d-axis characteristics," *IEEE Trans. Energy Convers.*, vol. 20, no. 1, pp. 88-97, Mar. 2005.

[20] S.-A. Tahan and I. Kamwa, "A two-factor saturation model for synchronous machines with saliency and saturation," *IEEE Trans. Energy Convers*., vol. 10, no. 4, pp. 609-616, Dec. 1995.

[21] E. Levi, "Saturation modeling in D-Q axis models of salient pole synchronous machines," *IEEE Trans. Energy Convers*., vol. 14, no. 1, pp. 44-50, Mar. 1999.

[22] *IEEE Guide for Synchronous Generator Modeling Practices and Applications in Power System Stability Analyses*, IEEE Std. 1110-2002, Dec. 2003.

[23] I. M. Canay, "Causes of discrepancies on calculation of rotor quantities and exact equivalent diagrams of the synchronous machine," *IEEE Trans. on Power App. and Syst.,* vol. 88, no. 7, pp. 1114-1120, Jul. 1969.

[24] J. L . Kirtley Jr., "On turbine-generator rotor equivalent circuits," *IEEE Trans. Power Syst.*, vol. 9, no. 1, pp. 262-271, Feb. 1994.

[25] I. Kamwa and P. Viarouge, "On equivalent circuit structures for empirical modeling of turbine-generators," *IEEE Trans. Energy Convers*., vol. 9, no. 3, pp. 579-592, Sep. 1994.

[26] F. Therrien, L. Wang, J. Jatskevich, and O. Wasynczuk, "Efficient explicit representation of AC machines main flux saturation in state-variable-based transient simulation packages," *Accepted for publication* in *IEEE Trans. Energy Convers.* (ID: TEC-00422-2012).

[27] U. M. Ascher and C. Greif, *A first course in numerical methods*, Philadelphia, PA: SIAM, 2011.

[28] H. Atighechi, S. Amini Akbarabadi, F. Therrien, and J. Jatskevich, "Average-value modeling of synchronous machine line-commutated converter using a constant-parameter voltage-behind-reactance interfacing circuit," in *Proc. Int. Conf. Power Syst. Transients*, Vancouver, BC, Canada, July 18-20, 2013.